Composite Structures 96 (2013) 75–81

Contents lists available at SciVerse ScienceDirect

Composite Structures

journal homepage: www.elsevier.com/locate/compstruct

Multi-objective optimization of a composite rotor blade cross-section

Swaroop B. Visweswaraiah, Hossein Ghiasi, Damiano Pasini, Larry Lessard *

Department of Mechanical Engineering, McGill University, Canada

ARTICLE INFO

Article history:
Available online 9 October 2012

Keywords:
Composite rotor blade
Target vector optimization
Multi-objective optimization
Pareto front

ABSTRACT

This paper deals with the optimization of the ply angles and the internal geometry of a composite helicopter blade with a D-spar internal construction. The design involves the simultaneous optimization of several conflicting objectives such as: attaining three stiffness parameters, minimizing the blade mass and the distance between the mass-center and the aerodynamic-center. Optimization methods with *a priori* and *a posteriori* articulation of preferences are used to solve the problem. Among the *a priori* approaches, the min–max approach is used to transform multiple objective functions into a single criterion which is optimized with Particle Swarm Optimization (PSO). Alternatively, the design problem is tackled using *a posteriori* approach by using our in-house Non-dominated Sorting Hybrid Algorithm (NSHA). The results obtained with NSHA demonstrate trade-off designs which could not be captured with the min–max approach. The multi-objective approach allows identifying a window of 10% adjustment in mass and 20% adjustment in the distance between the mass center and the aerodynamic center with no significant deviation from the target stiffness vector. Furthermore, we have observed that the target stiffness vector can be attained more easily if the internal geometry, besides the ply angles, is considered as a design variable.

1. Introduction

High stiffness-to-weight, strength-to-weight ratios and superior fatigue and dynamic properties are among crucial characteristics that a helicopter rotor blade should be designed for. Laminated composite structures can cater to such performance requirements provided that their material and geometry parameters are optimally designed. This can be a daunting task due to the interdisciplinary nature of the design problem, the presence of conflicting objectives and the number and nature of the design variables involved. This complexity has led to the use of hierarchical decomposition approaches [1] that allow modularization within the structural discipline and facilitate the interaction among hierarchical levels. The structural design of a blade is decomposed into an upper and a lower level [1,2] problem. At the upper level, the stiffness vector of the blade is treated as a variable that is adjusted to provide minimum vibration or maximum aeroelastic performance. At the lower level, which is the aim of this study, the lamination, material parameters and the cross-section geometry are optimized to provide the target stiffness vector determined at the upper level.

The cross-section design of a rotor blade requires simultaneously achieving several target stiffness parameters; however, pioneering studies are mainly focused on single-objective formulations [2]. The most popular technique is the min–max approach in which the maximum deviation from the target stiffness vector is minimized [4,5]. This technique yields only one solution and fails to capture other Pareto-optimal solutions. In addition, it cannot take into account other objectives, such as the structural mass and the distance between the aerodynamic center (AC) and the mass center (MC); yet, these are shown to play a crucial role in the blade performance [3]. A lower structural mass of the blade enhances the payload carrying capacity, while a shorter distance between the AC and MC facilitates reducing the pitching moments and benefits the aerodynamic performance. Leihong et al. [3] proposed to use a weighted-sum approach; however, this strategy requires assigning preferences by the user and yet fails to capture multiple optimal solutions on the Pareto front. In this study, a multi-objective optimization approach is proposed to find the Pareto front without the need to set *a priori* preferences on the objective functions.

After formulating the problem into a multi-objective optimization framework, an appropriate optimization algorithm must be selected. The design optimization of composite structures is often characterized by the presence of several local minima and discrete design variables. Particle Swarm Optimization (PSO) [5,6] and Genetic Algorithms (GAs) [4] are two common algorithms suitable for solving the lower-level problem of the blade design. This point was substantiated even by authors who opted to use other methods, such as the method of feasible directions [7]. Computational advantage and superior performance of the PSO over GA-based approaches and gradient-based approaches have been demonstrated

* Corresponding author. Address: 817 Sherbrooke West, MacDonald Engineering Building, Department of Mechanical Engineering, McGill University, QC, Canada H3A 2K6. Fax: +1 514 3987365.
E-mail address: larry.lessard@mcgill.ca (L. Lessard).

0263-8223/$ - see front matter © 2012 Elsevier Ltd. All rights reserved.
http://dx.doi.org/10.1016/j.compstruct.2012.09.031

on particular test cases [5,6]; however, such conclusion may not be generalized. To improve upon the high computational requirement and low convergence rate of these methods, several hybrid algorithms have been proposed [3,7], one of the most recent ones, namely NSHA [8], is used in this research.

Finally a realistic model of the structural behavior of the blade is required. The popular approach of modeling a composite blade as a box-beam inhibits the designer to examine the sensitivity of the blade performance to the cross-sectional geometrical parameters. Although small in number, the research works that opted for a realistic model of the blade have demonstrated that the ply angles and internal geometry parameters are crucial in efficient handling of the stiffness values and aerodynamic performance of a composite blade [3,7,8].

This work contributes towards the optimum design of a composite blade by demonstrating a design approach that differs from those in the literature in the following four aspects: (1) it uses a blade with a realistic airfoil cross-section and a variable internal geometry, rather than a simplified box-beam model; (2) it shows the impact of the internal geometry parameters on the target stiffness vector; (3) it proposes a multi-objective optimization approach that does not require *a priori* prioritization of the objectives; and (4) it considers mass and aerodynamic performance, besides the target stiffness vector, to clearly demonstrate the trade-off designs of the composite rotor blade.

These goals are achieved by first performing a target vector optimization using a min–max formulation and PSO, with and without inclusion of the cross-section geometry variables and with different fiber angle discretizations. Next, the multi-objective formulation of the target-stiffness problem is solved using NSHA [8]. This formulation allows optimization of other performance parameters, in addition to the target stiffness vector. Multiple solutions obtained by this approach are discussed to provide an insight into the conflicting behavior and the interaction between the stiffness components and the aerodynamic performance parameters.

2. Blade modeling

The complex geometry of the blade cross-section and the anisotropic nature of composite materials make accurate 3-D finite element modeling of a composite blade a challenging and time consuming task. As an alternative, a simplified approach is used that models the blade as an equivalent 1-D beam. The stress–strain relation and the cross-sectional stiffness matrix of the blade in this formulation is as follows:

$$\begin{bmatrix} N_x \\ M_y \\ M_z \\ T_x \end{bmatrix} = \begin{bmatrix} a_{11} & a_{12} & a_{13} & a_{17} \\ a_{12} & a_{22} & a_{23} & a_{27} \\ a_{13} & a_{23} & a_{33} & a_{17} \\ a_{17} & a_{27} & a_{37} & a_{77} \end{bmatrix} \begin{bmatrix} \varepsilon_x^0 \\ 1/\rho_y \\ 1/\rho z \\ \theta \end{bmatrix} \quad (1)$$

The diagonal terms of the stiffness matrix are of primary importance. The first diagonal term, a_{11}, represents the axial stiffness, while the others are shown in Fig. 1. The off-diagonal terms are referred to as elastic couplings. N_x in this equation represents the axial force, M_y and M_z are the flapwise and chordwise bending moments and T_x is the torsional moment. Correspondingly, ε_x^0 represents the axial strain, ρ_y and ρ_z are the curvatures around Y and Z axes and θ shows the shear strain. A computationally efficient in-house code is developed in MATLAB that calculates the stiffness matrix of a composite beam with an arbitrary cross-section using a combination of beam theory, plate theory and classical lamination theory [10–16]. Appendix A shows the principal equations used in this code.

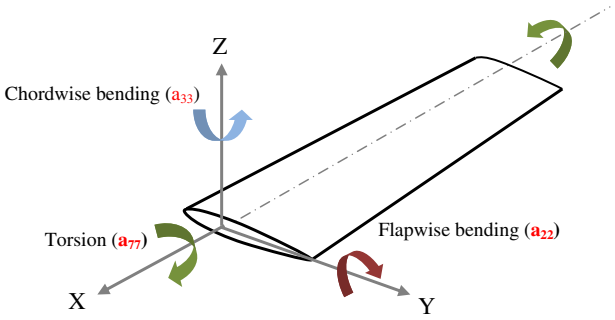

Fig. 1. Composite beam and co-ordinate system.

3. Composite blade optimization

A generic cross-section of a composite blade with a D-spar internal construction is shown in Fig. 2. The design vector includes discrete and continuous variables and consists of six ply angles (θ_1–θ_6), web distance from the leading edge (wd), and the inclination angle of the spar web (α_{web}). To account for different manufacturing conditions, the fiber angles are discretized in the range of 0°–90° with the increment of 10° (high precision manufacturing), 15° and 45° (low quality, non-expensive manufacturing). A symmetric layup is chosen in order to mitigate any warpage. The web distance, wd, is assumed to be continuous and ranges from 30% to 70% of the chord length so as to produce designs that are realistic and manufacturable. The spar web angle, α_{web}, is also a continuous variable ranging from −30° to 30°. A web inclination greater than 30° is not accepted as it can cause overly large resin-rich regions at the corners. The cross-sectional geometry, material properties and the target stiffness values used in this study are shown in Table 1. The target stiffness vector is the one used by Suresh et al. [5].

3.1. Problem formulation

While the literature on target stiffness design of composite blades entails mainly the use of a min–max approach, here four different formulations are proposed. They are referred as Cases 1–4.

3.1.1. Case 1

includes the traditional min–max approach where the objective is to minimize the maximum deviation from the target stiffness vector. The value of the min–max error represents the proximity of the stiffness vector of the current design to the target stiffness vector. Two sub-cases with dissimilar design variables are examined.

3.1.1.1. Case 1(a). considers only the ply angles as design variables. The web is kept constant at the vertical position at the distance of 0.35C (35% of the chord length) from the leading edge of the blade.

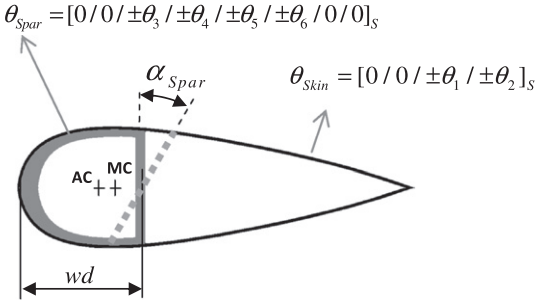

Fig. 2. Generic cross-section of a rotor blade with a D-spar construction.

Table 1
Airfoil geometry and graphite/epoxy material properties, target stiffness vector.

Airfoil profile	NACA0015	*Material properties of graphite/epoxy*	
Chord length, C (m)	0.3048		
Web-distance, wd	0.35C	$E1$ (GPa)	141.5
Target stiffness vector [5]		$E2$ (GPa)	9.8
EI_{yy}^{T} (N m^2)	39,767	$G12$ (GPa)	5.9
EI_{zz}^{T} (N m^2) about AC	82,916	Poisson's ratio, v	0.42
GJ^{T} (N m^2)	20,420	ρ (kg/m^3)	1445.4

The optimization problem is mathematically represented as follows:

$$\min_{\theta_i}\{\max\{f_j(\theta_i):\Theta^6\mapsto\Re;\quad i=1,\ldots,6;\quad j=1,2,3\}\}$$
$$S.T.:\Theta=\{\theta|-90^\circ\leqslant\theta=10k\ or\ 15k\ or\ 5k\leqslant 90;\quad k\in\Im\} \tag{2}$$

where the objective functions are defined as:

$$f_1=\left(\sqrt{\frac{(EI_{yy}-EI_{yy}^{T})^2}{(EI_{yy}^{T})^2}}*100\right)\quad f_2=\left(\sqrt{\frac{(EI_{zz}-EI_{zz}^{T})^2}{(EI_{zz}^{T})^2}}*100\right)\quad f_3=\left(\sqrt{\frac{(GJ-GJ^{T})^2}{(GJ^{T})^2}}*100\right) \tag{3}$$

3.1.1.2. Case 1(b). emphasizes the role of the internal geometry variables and considers both ply angles and the internal geometry parameters. The optimization problem here is formulated as follows:

$$\min_{\theta_i,\alpha_{spar},wd}\{\max\{f_j(\theta_i,\alpha_{spar},wd):(\Theta^6,\Re^2)\mapsto\Re;\ \ i=1,\ldots,6;\ j=1,2,3\}\}$$
$$S.T.\begin{cases}\Theta=\{\theta|-90^\circ\leqslant\theta=10k\ or\ 15k\ or\ 45k\leqslant 90^\circ;\ \ k\in\Im\}\\ \alpha_{spar}^{L}\leqslant\alpha_{spar}\leqslant\alpha_{spar}^{U}\\ wd^{L}\leqslant wd\leqslant wd^{U}\end{cases} \tag{4}$$

3.1.2. Case 2

describes situations where the achievement of certain components of the target stiffness vector is more important than the others; for instance, Bhadra et al. [17] showed that the bending stiffness at the root of a helicopter blade is more important than the torsional stiffness. In contrast, closer to the tip of the blade the torsional stiffness is more important than the bending stiffness. Assigning preferences to the objective functions requires information about the trade-off among three stiffness parameters, which does not exist in practice; therefore *a posteriori* approach is proposed to obtain a set of optimal solutions. The formulation of the problem is similar to Case 1(b) (Eq. (4)) with the exception of the objective function that is defined as follows:

$$\min_{\theta_i,\alpha_{spar},wd}\{f_j(\theta_i,\alpha_{spar},wd):(\Theta^6,\Re^2)\mapsto\Re;\quad i=1,\ldots,6;\quad j=1,2,3\} \tag{5}$$

3.1.3. Case 3

combines the min–max target stiffness problem with another performance parameter, the blade mass. Although several researchers considered mass as an objective, none has used *a posteriori* approach to establish the trade-off between the target stiffness and the blade mass. The formulation of the problem is similar to Eq. (4) with the objective being modified as follows:

$$\min_{\theta_i,\alpha_{spar},wd}\{\max\{f_j(\theta_i,\alpha_{spar},wd),\quad j=1,2,3\},mass(\theta_i,\alpha_{spar},wd)\}$$
$$:(\Theta^6,\Re^2)\mapsto\Re;\quad i=1,\ldots,6 \tag{6}$$

Not only the blade mass, but also the distance between MC and AC is crucial in the performance of a blade. The MC–AC distance must be minimized otherwise additional non-structural mass would be required to adjust the distance. Minimization of MC–AC distance is an objective considered in the next formulation of the blade design problem, Case 4.

3.1.4. Case 4

is similar to Case 3 but it requires minimizing the MC–AC distance. AC is assumed to be at 25% of the chord length.

3.2. Optimization methods

Among several formulations proposed in the previous section, only Case 1 converts the design problem into a single-objective optimization problem. All other formulations imply simultaneous optimization of multiple objectives. Since the relative priority of the objectives is unknown prior to solving the optimization problem, a multi-objective optimization method with *a posteriori* articulation of preferences is required. Such an optimization method is able to provide several optimum solutions and illustrate the trade-off among the objective functions. This section explains the single- and multi-objective optimization techniques used to solve Cases 1–4 formulated in previous section.

3.2.1. Particle Swarm Optimization (PSO)

Particle Swarm Optimization [18] is a multi-agent search technique based on the behavior of a swarm. A swarm, composed of several entities called "particles", explores the design space of a problem seeking the optimum value of a single objective function. PSO is suitable for a combinatorial problem characterized by the presence of local minima and discrete design variables such as the problem in hand; however, it is limited to single-objective problem and hence Case 1 is the only formulation in this study that allows the use of this optimization method. A swarm consisting of 50 particles is found to be the minimum swarm size that returns an acceptable convergence for the problem in hand. The inertia weight that controls the trade-off between the global and the local exploration ability of the swarm is linearly decreased from 0.8 to 0.1. Finally, the cognitive/acceleration constants that represent the relative importance of position of the particle to the position of the swarm are taken as two.

3.2.2. Non-dominated Sorting Hybrid Algorithm (NSHA)

To handle multiple objectives without assigning any priority or preference to the objectives, a multi-objective hybrid algorithm developed by Ghiasi et al. [8] is used. This technique, known as Non-dominated Sorting Hybrid Algorithm (NSHA), is a modified version of NSGA-II [19], NSHA starts with a randomly generated population with a user-defined size. Using this initial population, a few generations of NSGA-II are carried out. The local search is activated only after all the individuals of the current population are located at the first non-domination front. When activated, the local search operates only on a subset of the current population and a subset of design variables. In order to locally improve good solutions in the current population of NSGA-II, a simplex is generated around each selected solution and a local search based on Nelder–Mead simplex method [20] is executed. The locally optimized solutions replace the original ones and the improved population is used for the next few generations by NSGA-II.

It is shown that NSHA increases the convergence rate of NSGA-II and improves the spread of the solutions while offers simplicity, modularity and independency to user-defined parameters [8] similar to NSGA-II. In addition to handling multiple objectives without prioritization, NSHA is able to capture optimum solutions at the presence of multiple local optima and discontinuity within the design space, hence properly fitting the problem at hand.

The minimum initial population for NSHA that results in a reasonable convergence rate and preserves the diversity of the

population, is found by trial-and-error and is set to 400 points. The algorithm is found to converge after approximately 50,000 function evaluations. Other user-defined parameters in NSHA are adjusted to recommended values in [8]. In both algorithms, the optimization process was initiated at random. Each case is optimized five times and the best results of all the runs are reported in the following section.

4. Results and discussion

The optimization algorithms described in the previous section are used to solve the four proposed cases formulated in Section 3.1. The optimum solutions are presented, contrasted and discussed in this section.

4.1. Target stiffness design using min–max approach (Case 1)

The min–max target stiffness design problem, formulated in Section 3.1, is solved using PSO with and without consideration of the internal geometry parameters. The results presented in Table 2 shows that the average deviation from the target stiffness vector (i.e. the value of the objective function, f) can be as high as 7% when the internal geometry parameters are not considered; however, the target objective is achieved with a deviation less than 1.2% when the internal geometry parameters are considered. A more detailed analysis of the results reveals that the stiffness vector is less sensitive to the web angle than to the web distances, which confirms the parametric studies published in [9]. The difference between the optimum cross-sectional geometry achieved in Case 1(b) and the base-line geometry in Case 1(a) is shown in Fig. 3. Lower deviation from the target stiffness vector in Case 1(b) is accompanied by an increase in the spar size and consequently an undesired increase in mass. The clear trade-off between the two aforementioned objectives confirms that structural benefits can be gained if the target stiffness design is combined with the minimum mass design in a multi-objective optimization framework. Case 3 is an effort to address this issue.

The results also show that among different discretizations schemes, the one with 10° increment yielded the lowest deviation from the target stiffness vector. The level of fiber angle discretization can be evaluated as a measure representing the manufacturability of the design. From the manufacturability point-of-view, coarse ply angle discretizations are preferred to the fine ones as the placement of fibers in large number of different angles is a tedious task. Table 2 shows that fine ply angle discretizations generally return a lower deviation from the target stiffness parameters and a lower mass for the structure. Fine discretization of the ply angles is also beneficial from an optimization standpoint, as it allows better exploration of the design space and improves the convergence rate of the algorithm. The remainder of the results presented in this paper use 10° increments for the ply-angles.

Table 2
Optimum solutions for Case 1(a) and 1(b).

	Without internal geometry variables Case 1(a)			With internal geometry variables Case 1(b)		
	Discretization			Discretization		
Design variables	10°	15°	45°	10°	15°	45°
θ_1 (°)	40	45	45	50	60	45
θ_2 (°)	80	75	45	80	90	45
θ_3 (°)	30	15	45	30	45	90
θ_4 (°)	30	30	0	90	75	45
θ_5 (°)	20	30	0	60	90	0
θ_6 (°)	30	30	45	0	0	90
α_{spar} (°)	0			−7.06	−5.63	−0.50
wd as %C	0.35			0.43	0.47	0.43
Computation time (s)	151.1	186.9	276.0	166.4	247.2	194.1
Mass (kg/m)	2.48	2.48	2.48	2.68	2.79	2.68
Objective function (f)	3.75	5.92	7.09	0.11	0.35	1.18
Number of Iterations	35	42	50	41	60	46

4.2. Target stiffness design using NSHA (Case 2)

While the trade-off between stiffness tailorability, blade mass and manufacturability was observed in the results of Case1, no comment could be made concerning the trade-off among the three components of the stiffness vector. Case 2 examines this trade-off by individually and simultaneously minimizing the deviation from three target stiffness values using NSHA.

Fig. 4 shows the set of optimal solutions found by NSHA. This figure confirms the possibility of designing a blade that can achieve all three components of the target stiffness vector with less than 0.5% deviation from the target values. The traditional min–max approach returns only one point on the Pareto surface; however the Pareto surface shown in Fig. 4 gives an overview of other possible designs. This approach can help adjusting the most important stiffness parameter close to the target value with a predictable loss in other stiffness parameters; it can also be beneficial when designing an intrinsically smart composite blade with variable stiffness along the blade span.

Fig. 5 shows all the optimum solutions sorted by deviation from the chordwise target stiffness (f2). The majority of the solutions have a very low deviation from chordwise target stiffness (small value for f2) and relatively high deviation in other stiffness components (f1 and f3). We mark these optimum solutions as "Set 1". An attempt to reduce the deviation from torsional stiffness (f3) causes drastic changes in all stiffness components. This can be attributed to a shift from one local optimum to another. The shift in local minima of f3 corresponds to severe changes in stacking sequence but a very small change in position and angle of the web. Another distinct set of solutions (shown as "Set 2" in this figure) corresponds to solutions with low f1 and f3 values but higher f2 values. Traditional min–max approach can find only a single solution to this problem overlooking the rest of the spectrum. Most of the solutions in Set 2 exhibit less deviation from target flapwise and torsional stiffness than the traditional min–max solution. NSHA gives the opportunity to the designer to see other possible solutions and to select the optimum design according to the situation. For instance, solutions in Set 1 can be better than solutions in Set 2 for particular applications where torsional stiffness is more important than flapwise and chordwise bending stiffness.

From the manufacturing point of view, solutions in Set 1 are more favorable because they are less sensitive to the design parameters. Set 2 is also relatively stable but less than Set 1; however, it corresponds to a min–max error less than the one achievable in Set 1. The final design is not only a trade-off among three target stiffness parameters but also a trade-off between manufacturability and target stiffness vector. A sensitivity analysis carried out on the solution in Set 1 shows that the objectives are generally more sensitive to geometrical design variables than fiber angles, with the web distance being the most influential variable.

4.3. Target stiffness vs. mass (Case 3)

The analysis of the results from Case 1 suggests that there is a trade-off between mass and level of achieving the target stiffness vector. Case 3, which is solved by NSHA, is formulated to demonstrate this trade-off. The most interesting observation is the clear exchange between mass and maximum deviation from the target stiffness values shown in Fig. 6. This figure shows that for the particular blade studied here, reducing the deviation from the target

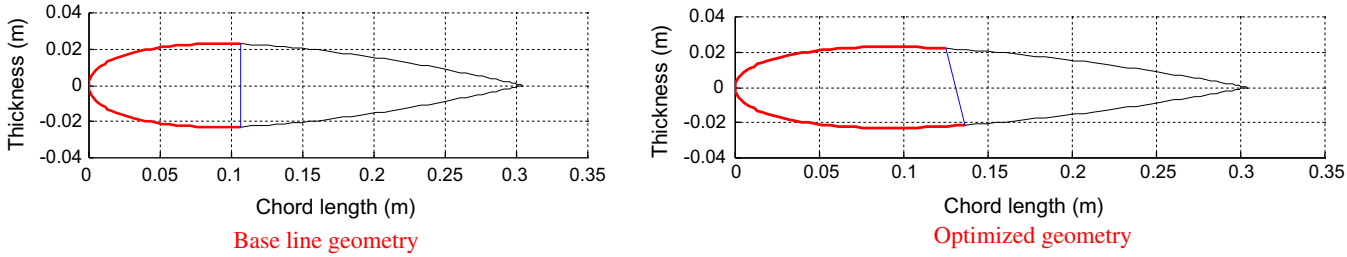

Fig. 3. The baseline geometry yields a min–max error of 3.75%; while the optimized geometry yields a min–max error of 0.11%.

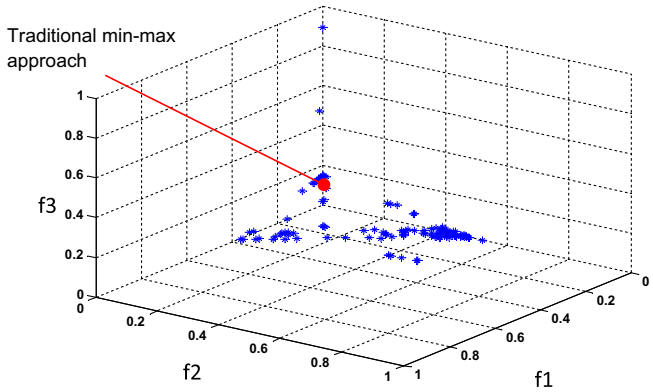

Fig. 4. Pareto-front for Case 3 shows that a trade-off exists among three target stiffness parameters, which could not be captured by traditional min–max method.

stiffness from 5% to 2% increases the mass of the blade by around 300 g. The most influential design parameter in this trade-off is the web-distance, which is also responsible for the significant increase of mass seen in Fig. 6. The increase in mass corresponds to the relocation of the web from 0.45C to 0.37C. The target stiffness vector is achieved with a lower error, when the web is located at the distance of approximately 0.45C from the leading edge; however, designs with lower masses are achieved at lower web distances. Web distance not only affects the mass, but also is crucial in the aerodynamic performance of the blade; therefore, it is necessary to see the trade-off between stiffness vector and aerodynamic performance of the blade. This relation is studied in Case 4.

4.4. Target stiffness vs. MC–AC distance (Case 4)

The results of the simultaneous optimization of stiffness and aerodynamic performance are shown in Fig. 7. The trade-off between MC–AC distance and the maximum deviation from target stiffness vector is apparent. Similar to Case 3, the web distance is the most influential design parameter and is responsible for the discontinuity of the data. Fig. 7 also shows that a decrease in MC–AC distance from 0.026% to 0.022% results in only a marginal penalty in stiffness, while reducing the MC–AC distance below this value corresponds to a large deviation from the target stiffness vector (around 3%). Since MC–AC distance is usually adjusted by adding non-structural masses, the results in Case 3 and Case 4 can be combined to design a blade with minimum total weight and maximum aerodynamic performance while meeting the assigned stiffness requirements.

5. Conclusion

The lower-level design optimization problem of a helicopter rotor blade has been solved using two different formulations: (1) the single-objective min–max approach for the target vector optimization utilizing Particle Swarm Optimization, and (2) a multi-objective formulation utilizing multi-objective GA-based hybrid algorithm called NSHA. The multi-objective formulation involves simultaneously minimizing the structural mass of the blade, the MC–AC distance and the deviation from three target stiffness parameters. A realistic model of a blade with airfoil cross-section has been created to study the effect of internal geometry variables and ply angles on the structural and aerodynamic performance of the blade.

The first set of results obtained from a single-objective min–max optimization has demonstrated the crucial role of internal geometry parameters and ply-angle discretization on the blade stiffness. Adjustment of the internal geometry variables obtained with a 10° ply-angle discretization has yielded a blade whose stiffness vector differed from the target stiffness vector by only 0.11%. Further analysis of the results has shown that the internal geometry variables are more crucial than ply-angles; thus the inclusion of these parameters into the design problem greatly facilitates achieving the target stiffness vector. This study also confirmed that lowering the deviation from the target stiffness vector accompa-

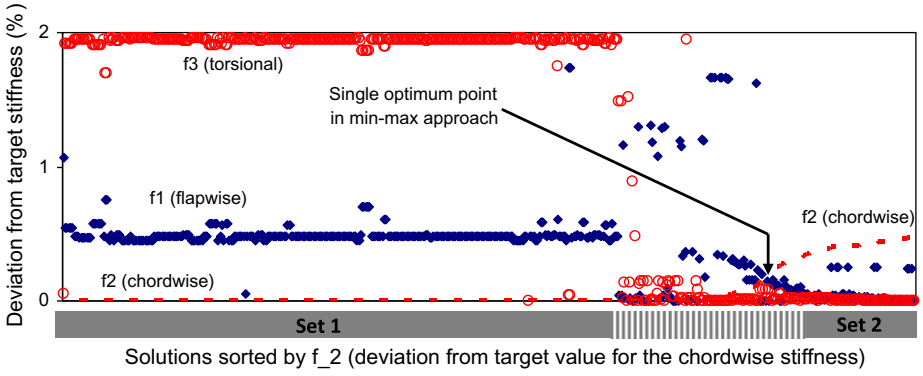

Fig. 5. Comparison of the optimum solutions found by a multi-objective optimization approach and the single solution achieved by the traditional min–max approach.

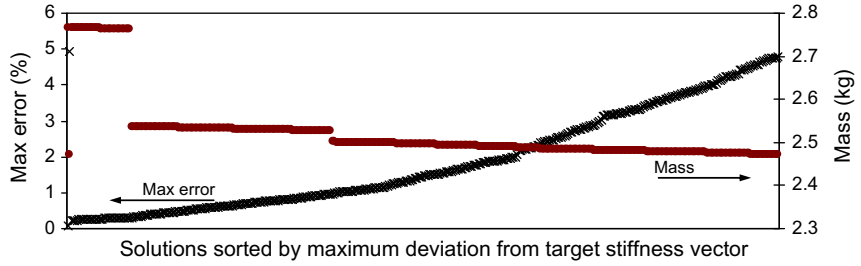

Fig. 6. The trade-off between achieving target stiffness (max-error) and the total mass of the blade captured by the multi-objective optimization approach.

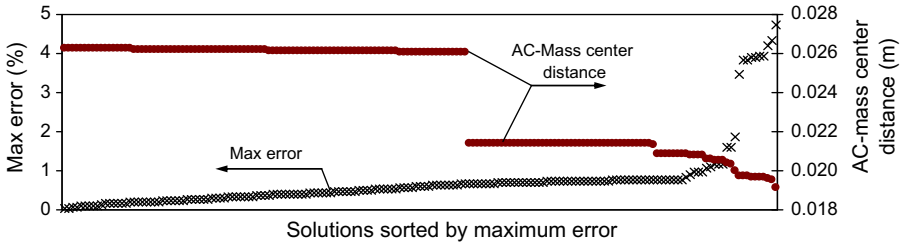

Fig. 7. Reducing the distance between the aerodynamic center and the mass center causes an increase in total mass of the blade.

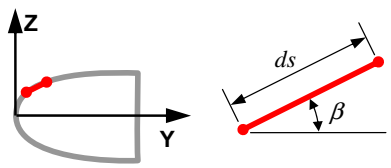

Fig. A1. D-spar coordinate system.

nies an increase in the blade mass, hence the simultaneous minimization of these parameters is recommended.

In addition, multi-objective optimization of a composite blade was carried out in order to highlight the trade-offs among three stiffness components, mass and aerodynamic performance of the blade. Pareto frontiers were found for these trade-off designs. The analysis of the results showed that the simultaneous consideration of mass and target stiffness can give a window of up to 11% adjustment in structural mass without a significant deviation from the target stiffness vector. This is particularly beneficial to the design of a helicopter blade, where minimizing the structural mass mitigates the dynamic stresses. Similarly, including the aerodynamic performance in the target stiffness optimization process provides opportunity to vary the MC–AC distance by up to 20%; this choice can reduce the weight of non-structural mass usually added for the adjustment of the MC–AC distance.

Appendix A. Blade modeling

The blade cross-sectional stiffness matrix shown in Eq. (2) is computed using closed-form expressions developed in [13]. A composite blade is modeled as a slender thin-walled beam (thickness-to-chord ratio and chord-to-length ratio less than 0.1). Assuming a negligibly small thickness-to-curvature ratio, a small segment of such one-dimensional beam is considered as a flat composite laminate, as shown in Fig. A1.

The stress–strain relation for the flat composite laminate is as follows:

$$N_i = A_{ij}\varepsilon_j^\circ + B_{ij}k_j; \quad M_i = B_{ij}\varepsilon_j^\circ + D_{ij}k_j; \quad i = 1,2,6$$

$$\sigma_i = \sum_{j=1,2,6} Q_{ij}\varepsilon_j, i = 1,2,6$$

where N and M are force and moment resultants and indices 1, 2 and 6 shows axial, transverse and shear directions, respectively. Matrix A, D and B are axial, bending and coupling stiffness matrices which are defined as follows (see Refs. [10–16] for details).

$$[A_{ij}, B_{ij}, D_{ij}] = \int_{thickness} Q_{ij}[1, z, z^2]dz, \qquad i = 1,2,6, \quad j = 1,2,6$$

Using linear elasticity theory, overall stiffness of the blade section can be obtained by summing the stiffness of these segments over the entire section. Each term in cross-sectional stiffness matrix in Eq. (2) can be calculated as shown below:

$$a_{11} = \int K_{11}ds \qquad a_{22} = \int [K_{11}y^2 + 2yK_{14}Cos\beta + K_{44}(Cos\beta)^2]ds$$

$$a_{33} = \int [K_{11}z^2 - 2zK_{14}Sin\beta + K_{44}(Sin\beta)^2]ds \qquad a_{77} = \delta_c \int \psi K_{23}ds + 2\int K_{53}ds$$

$$a_{12} = \int [K_{11}y + K_{14}Cos\beta]ds \qquad a_{13} = \int [K_{11}z - K_{14}Sin\beta]ds$$

$$a_{17} = \int K_{13}ds \qquad a_{23} = \int [K_{11}yz - yK_{14}Sin\beta + zK_{14}Cos\beta - K_{44}Sin\beta Cos\beta]ds$$

$$a_{27} = \int [K_{13}y + K_{43}Cos\beta]ds \qquad a_{37} = \int [K_{13}z - K_{43}Sin\beta]ds$$

where reduced stiffness, K, is defined as follows:

$$K_{11} = A_{22} - A_{12}^2/A_{11} \quad K_{14} = B_{22} - A_{12}B_{12}/A_{11}, \quad K_{44} = D_{22} - B_{22}^2/A_{11}$$

$$K_{13} = 2\left(A_{26} - \frac{A_{12}A_{16}}{A_{11}}\right)\frac{\Omega}{\alpha} + 2\left(B_{26} - \frac{A_{12}B_{16}}{A_{11}}\right), \qquad K_{23} = 2\left(A_{66} - \frac{A_{16}^2}{A_{11}}\right)\frac{\Omega}{\alpha} + 2\left(B_{66} - \frac{A_{16}B_{16}}{A_{11}}\right)$$

$$K_{43} = 2\left(B_{26} - \frac{B_{12}A_{16}}{A_{11}}\right)\frac{\Omega}{\alpha} + 2\left(D_{26} - \frac{B_{12}B_{16}}{A_{11}}\right), \qquad K_{23} = 2\left(B_{66} - \frac{B_{16}A_{16}}{A_{11}}\right)\frac{\Omega}{\alpha} + 2\left(D_{66} - \frac{B_{16}^2}{A_{11}}\right)$$

$$\alpha = \oint ds, \quad \Omega = 1/2 \oint Sds, \quad \psi = 2\Omega/\beta$$

References

[1] Walsh JL, Young KC, Pritchard JI, Adelman HM, Mantay WR. Integrated aerodynamic/dynamic/structural optimization of helicopter rotor blades using multilevel decomposition. Technical Report 3465, NASA; January 1995.
[2] Ganguli R. Survey of recent developments in rotorcraft design optimization. J Aircr 2004;41(3).

[3] Li Leihong, Volvoi Vitali V, Hodges DH. Cross-sectional design of composite rotor blades. J Am Helicopter Soc 2008:10.
[4] Murugan MS, Suresh S, Ganguli R, Mani V. Target vector optimization of composite box beam using real-coded genetic algorithm: a decomposition approach. Struct Multidiscip Optim 2007;33:131–46.
[5] Suresh S, Sujit PB, Rao AK. Particle swarm optimization approach for multi-objective composite box-beam design. Compos Struct, vol. 81. Elsevier; 2007. p. 598–605.
[6] Kathiravan R, Ganguli R. Strength design of composite beam using gradient and particle swarm optimization. Compos Struct 2007;81:471–9.
[7] Paik J, Volovoi VV, Hodges DH. Cross-sectional sizing and optimization of composite blades. In: Proceedings of the 43rd AIAA/ASME/ASCE/AHS/ASC structures, structural dynamics, and materials conference. Denver, Colorado: AIAA 2002-1322; April 22–25, 2002. p. 601–10.
[8] Ghiasi H, Pasini D, Lessard L. A non-dominated sorting hybrid algorithm for multi-objective optimization of engineering problems. Eng Optimiz 2011;43(1):39–59.
[9] Visweswaraiah S, Pasini D, Lessard L. A study of the effect of geometry changes on the structural stiffness of a composite D-spar. In: ASME 2010 international design engineering technical conferences and computers and information in engineering conference (IDETC/CIE2010), Paper no. DETC2010-28730; p. 51–58.
[10] Smith Edward C, Chopra Inderjit. Formulation and evaluation of an analytical model for composite box-beams. J Am Helicopter Soc 1991.
[11] Berdichevsky VL. Variational-asymptotic method of constructing a theory of shells. J Appl Math Mech (Engl Trans Prikladnaya Matematika i Mekhanika) 1979;43(4):664–87.
[12] Hodges DH. Non-linear composite Beam theory. Reston: AIAA; 2006.
[13] Librescu Liviu, Song Ohseop. Thin-walled composite beams. Theory and application. Springer; 2006.
[14] Jung Sung Nam, Nagaraj VT, Chopra Inderjit. Refined structural model for thin- and thick walled composite rotor blades. AIAA J 2002;40:105–16.
[15] Kollar LaszloP, Springer GeorgeS. Mechanics of composite structures. Cambridge University Press; 2003.
[16] Jung Sung Nam, Park Il-Ju, Shin Eui Sup. Theory of thin-walled composite beams with single and double-cell sections. Composites Part B 2007;38:182–92.
[17] Bhadra S, Ganguli R. Aeroelastic optimization of a helicopter rotor using orthogonal array – based metamodels. AIAA J 2006;44(9):1941–51.
[18] Kennedy J, Eberhart RC. Particle swarm optimization. In: Proceedings of the fourth IEEE international conference on neural networks; 1995. p. 1942–48.
[19] Deb K, Pratap A, Agarwal S, Meyarivan T. Fast and elitist multi-objective genetic algorithm: NSGA-II. IEEE Trans Evol Comput 2002;6(2):182–97.
[20] Nelder JA, Mead R. Simplex method for function minimization. Comput J 1965;7(4):308–13.